Latin American Journal of Solids and Structures
www.lajss.org

Strand Tension Control in Anchor Span for Suspension Bridge Using Dynamic Balance Theory

Abstract

Strand tension control is essential in suspension bridge safety. However, few quantitative studies have examined the bending rigidity and boundary condition behavior of strands in the anchor span of suspension bridges because of their special structure and complex configuration. In this paper, a new calculation method for strand tension is explored by using dynamic balance theory to determine the effect of bending rigidity and boundary conditions. The accuracy and effectiveness of the proposed method are tested and confirmed with verification examples and application on Nanxi Yangtze Suspension Bridge in China. The results indicated that only low-order frequency calculation could be used to calculate the strand tension without considering the effect of bending rigidity to ensure control accuracy. The influence of bending rigidity on the control precision is related to the tension and the length of the strands, which is significantly determined by the specific value between the stress rigidity and the bending rigidity. The uncertain boundary conditions of the anchor span cable, which are fixed between consolidated and hinged, also have a major effect on the control accuracy. To improve the accuracy of strand tension control, the least squares method is proposed during the tension construction control of the anchor span. This approach can significantly improve the accuracy of the tension control of the main cable strand. Some recommendations for future bridge analysis are provided based on the results of this study.

Keywords

Suspension bridge; dynamic balance method; bending rigidity; strand tension control; frequency method; least squares method.

Da Wang [a]
Wei Zhang [b]
YongMing Liu [c]
Yang Liu [d*]

[a,d] School of Civil Engineering and Architecture, Changsha University of Science & Technology, Changsha 410114 PR China
[b] Department of Civil and Environmental Engineering, University of Connecticut, Storrs, CT 06269, USA
[c] School for Engineering of Matter, Transport & Energy, Arizona State Univ., AZ 85281, USA

Corresponding author:
*yxwang2006@yeah.net

http://dx.doi.org/10.1590/1679-78252519

Received 08.10.2015
In revised form 13.03.2016
Accepted 14.04.2016
Available online 21.04.2016

1 INTRODUCTION

During the erection of strands of a main cable in a suspension bridge, shape control of the main cable is mainly for the mid-span and side-span, while the inner tension control of the cable is mainly

for the strand of the main cable in the anchor span. In the structure, the spatial position of the splay saddle is directly affected by the tension control accuracy of the anchor span, while the linear position of the side-span structure and the mid-span are directly affected by the spatial position of the splay saddle. Furthermore, large deviations in the anchorage span cause the structure of anchoring force to be insufficient, thereby endangering the structure. Apparently, strand tension and spatial position are the two most important components in monitoring the main cable of a suspension bridge during its construction. The former is particularly important for the anchor span, and the latter is important for the middle and side spans. However, the structural linear position is decided by the force; thus, the former has a significant influence on the latter (Xu and Huang, 2002; Kreis and Andre, 2005; Yau, 2013; Wang et al., 2014). For the suspension bridge, the main cable consists of almost 100 strands, and the internal force of the main cable is equivalent to thousands of tons. Although a slight deviation is observed in the tension calculation of the strand, the accumulative deviation cannot be ignored. Therefore, large deviations in strand tension in the anchor span would lead to insufficient anchoring forces and result in potentially catastrophic failures (Wang et al., 2014; Loh and Chang, 2006; Cho et al., 2012). Meanwhile, tension control accuracy of the anchor span has a significant effect on the safety of a structure both during construction and service (Song et al., 2001; Geier et al., 2009; Fang and Wang, 2012). Therefore, the strand tension control of the anchor span is one of the most important tasks during strand construction of suspension bridges.

At present, direct and indirect methods are the two main strand tension control methods. The direct method involves performing direct measurement using load measurement devices, whereas the indirect method performs an estimation based on the strand vibration. Direct methods measure strand tension by using a load cell or a pressure meter installed at the outset of a strand (Cho et al., 2012). Although the direct method is accurate and straightforward, load measurement devices are costly and fragile (Song et al., 2001; Wang et al., 2015); for example, approximately 100 strands are arranged in each anchor span of a long-span suspension bridge, which makes these strands difficult to arrange on all anchoring points. To alleviate this problem, the indirect method was developed using vibration frequency of the strand, which is widely used in practice. However, the indirect method is easily affected by boundary conditions and bending rigidity (Ni, 2002; Riceiardi and Saitta, 2008; Liu and Liu, 2010; Choi and Park, 2011; Li et al., 2011). Many studies were conducted for cable tension control of cable-stayed bridges (Loh and Chang, 2007; Hua et al., 2009; Ye et al., 2012), and a few conclusions could be taken as references for the strand tension control in the anchor span of suspension bridges. Although the structure characteristics between the strands in suspension bridges and the cables in cable-stayed bridges are similar, a detailed investigation showed that the former was shorter and stiffer, whereas the latter was longer and more flexible; references may be valuable for the latter but may not be directly used by the former. In addition, a notable detail is that accurate identification can be obtained by considering the effect of bending rigidity and boundary conditions (Ricciardi and Saitta, 2008; Zuo and Li, 2011). Strand tension control in suspension bridges needs further investigation.

Based on the preceding brief review, existing analysis methodologies usually focus on cable tension control of cable-stayed bridges. To improve the accuracy of strand tension control in the anchor span of these bridges, this study explores a new calculation method based on dynamic

balance theory, considering the effect of the bending rigidity and the boundary conditions in particular. A numerical simulation was conducted and examples were verified to investigate the effectiveness of the proposed method. Then, the proposed method was applied to the strand tension control in a long-span suspension bridge, and the effectiveness was tested with the field data based on the arranged sensors and the true value of the design. Some conclusions and recommendations for future strand tension control of suspension bridges are given based on the method.

2 DYNAMIC MODEL OF STRAND

2.1 Model of Strand Vibration

The strand of the main cable in the anchor span of a suspension bridge consists of multiple steel wires. Thus, the strands possess a certain bending rigidity. When we analyze the strand vibration included in the bending rigidity, we can denote the length of the cable as L, the angle of inclination as θ, the mass as m, the bending rigidity as EI, and the tension as T. The internal tension T remains unchanged when the cable vibrates slightly, as shown in Figure 1(a).

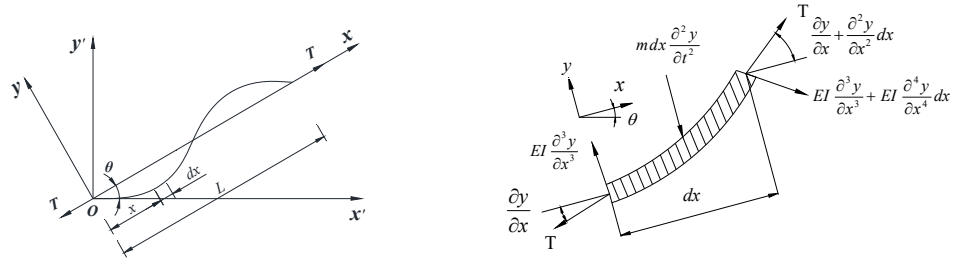

(a) Strand vibration model (b) Infinitesimal section model

Figure 1: Models of strand vibration and infinitesimal section.

To analyze the vibration equation of the cable, a section is randomly taken from within the length of the strand in an ideal state for analysis, as shown in Figure 2(b). The following can be deduced by establishing the dynamic balance equation in the y direction, as shown in Figure 2(b):

$$T\sin(\frac{\partial y}{\partial x}+\frac{\partial^2 y}{\partial x^2}dx)-T\sin(\frac{\partial y}{\partial x})-m\frac{\partial^2 y}{\partial t^2}dx=(EI\frac{\partial^3 y}{\partial x^3}+EI\frac{\partial^4 y}{\partial x^4}dx)\cos(\frac{\partial y}{\partial x}+\frac{\partial^2 y}{\partial x^2}dx)-EI\frac{\partial^3 y}{\partial x^3}\cos(\frac{\partial y}{\partial x}) \tag{1}$$

If the corner is infinitesimal when the strand vibrates slightly, then

$$\begin{cases}\sin(\dfrac{\partial y}{\partial x})\approx\dfrac{\partial y}{\partial x}\\ \sin(\dfrac{\partial y}{\partial x}+\dfrac{\partial^2 y}{\partial x^2}dx)\approx\dfrac{\partial y}{\partial x}+\dfrac{\partial^2 y}{\partial x^2}dx\end{cases} \tag{2}$$

and

$$\begin{cases} \cos(\dfrac{\partial y}{\partial x}+\dfrac{\partial^2 y}{\partial x^2}dx)\approx 1 \\ \cos(\dfrac{\partial y}{\partial x})\approx 1 \end{cases} \tag{3}$$

Equation (4) can be deduced by substituting Equations (2) and (3) into (1), i.e.,

$$EI\frac{\partial^4 y}{\partial x^4}-T\frac{\partial^2 y}{\partial x^2}+m\frac{\partial^2 y}{\partial t^2}=0 \tag{4}$$

and if

$$y(x,t)=\varphi(x)\eta(t) \tag{5}$$

The following can be deduced by substituting Equation (5) into Equation (4):

$$EI\frac{\varphi^{(4)}}{\varphi}-T\frac{\varphi''}{\varphi}=-m\frac{\eta''}{\eta} \tag{6}$$

To establish Equation (6), we set both sides of the equation to be equal to the same constant c, i.e.,

$$EI\frac{\varphi^{(4)}}{\varphi}-T\frac{\varphi''}{\varphi}=-m\frac{\eta''}{\eta}=c \tag{7}$$

The following can be deduced by breaking down Equation (7):

$$\begin{cases} \eta''(t)+\dfrac{c}{m}\eta(t)=0 \\ EI\varphi^{(4)}(x)-T\varphi''(x)-c\varphi(x)=0 \end{cases} \tag{8}$$

The following can be deduced by solving the first equation in Equation (8):

$$\eta(t)=A\cos\omega t+B\sin\omega t \tag{9}$$

where $\omega=\sqrt{\dfrac{c}{m}}$ is the circular frequency of the natural vibration of the strand.

The following can be deduced by solving the second equation in Equation (8):

$$\varphi(x)=C\sin\delta x+D\cos\delta x+E\sinh\xi x+F\cosh\xi x \tag{10}$$

where

$$\begin{cases} \delta=\sqrt{\sqrt{\alpha^4+\dfrac{\beta^4}{4}}-\dfrac{\beta^2}{2}} & \alpha^4=\dfrac{\omega^2 m}{EI} \\ \xi=\sqrt{\sqrt{\alpha^4+\dfrac{\beta^4}{4}}+\dfrac{\beta^2}{2}} & \beta^2=\dfrac{T}{EI} \end{cases} \tag{11}$$

The pending unknown parameters A, B, C, D, E, and F in Equations (9) and (10) are determined by the boundary and initial conditions of the strand. The strand model with general boundary conditions can be simplified, as shown in Figure 2.

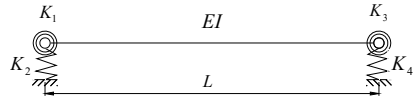

Figure 2: Strand model with general boundary conditions.

In Figure 2, K_1 and K_3 are the rotating restraint rigidity on both ends of the strand. When K_2 and K_4 are the vertical restraint rigidity on both ends of the strand, the boundary conditions of the strand are

$$\begin{cases} EI\dfrac{\partial^2\varphi(x)}{\partial x^2}\Big|_{x=0} = K_1\varphi'\big|_{x=0} & EI\dfrac{\partial^3\varphi(x)}{\partial x^3}\Big|_{x=0} = -K_2\varphi\big|_{x=0} \\ EI\dfrac{\partial^2\varphi(x)}{\partial x^2}\Big|_{x=L} = -K_3\varphi'\big|_{x=L} & EI\dfrac{\partial^3\varphi(x)}{\partial x^3}\Big|_{x=L} = K_4\varphi\big|_{x=L} \end{cases} \tag{12}$$

Parameters C, D, E, and F are obtained from the jointly established Equations (11) and (12), which have non-zero solutions, to solve the relational equation between the frequency and the strand tension.

2.2 Boundary Conditions

2.2.1 Hinged on Both Ends

In the calculation model shown in Figure 2, when both ends are hinged under boundary conditions, the corresponding restraint rigidity of the boundary is

$$\begin{cases} K_1 = K_3 = 0 \\ K_2 = K_4 = \infty \end{cases} \tag{13}$$

The following can be deduced by establishing and solving Equations (12) and (13):

$$T = \frac{4mL^2}{k^2}\cdot f_k^{\,2} - \frac{k^2\pi^2}{L^2}\cdot EI \tag{14}$$

where f_k in the equation is the frequency of order k when the strand vibrates, and $f_k = \dfrac{\omega_k}{2\pi}$.

2.2.2 Consolidated on Both Ends

In the calculation model shown in Figure 2, when both ends are consolidated under boundary conditions, the corresponding restraint rigidity of the boundary is

$$\begin{cases} K_1 = K_3 = \infty \\ K_2 = K_4 = \infty \end{cases} \tag{15}$$

The following can be deduced by establishing and solving Equations (12) and (15):

$$2 + \frac{\xi^2 - \delta^2}{\xi\delta} \sin \delta L \sinh \xi L - 2 \cos \delta L \cosh \xi l = 0 \tag{16}$$

Equation (16) is a hidden expression and can be solved by using Matlab.

3 VERIFICATION OF EXAMPLES

To verify the calculation accuracy and effectiveness of the proposed method, four strands were taken as the verified examples, and hinged boundary conditions were considered during the calculation process, as shown in Figure 3.

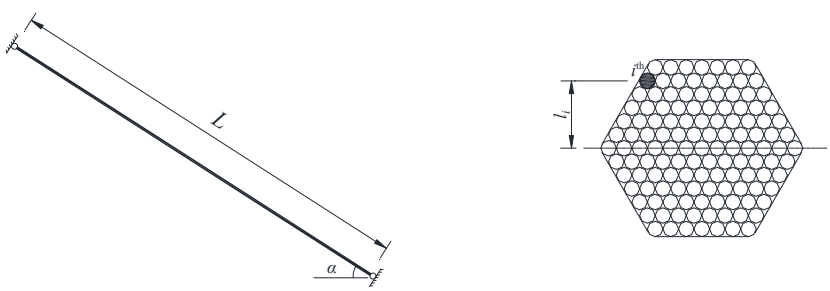

(a) Calculation model of the strand (b) Section of the strand

Figure 3: Model and section of the strand.

As indicated in Figure 3, the strand with a high internal tension can be taken as a beam (Song et al., 2001; Wang et al., 2015), and the bending rigidity of strand can be expressed as follows:

$$\begin{aligned} EI &= EI_i + A_i \cdot l_i^2 \\ &= \sum_{i=1}^{n} \frac{\pi D_i^4}{64} + A_i \cdot l_i^2 \end{aligned} \tag{17}$$

where E is the Young's modulus of the steel wire, I is the moment of inertia for the strand, I_i is the moment of inertia for the i^{th} high strength galvanized steel wire, D_i is the diameter of the i^{th} high-strength galvanized steel wire, and l_i is the distance from the center of the i^{th} steel wire circle to the centroidal axis of the strand section.

The area of the section of the strand is the sum of that of the high-strength galvanized steel wire, and the mass of the strand per meter can be obtained as follows:

$$m = \rho A = \rho \sum_{i=1}^{n} A_i \tag{18}$$

where A is the area of the strand, A_i is the area of each high-strength galvanized steel wire, and ρ is the density of the high-strength galvanized steel wire.

A combination of Equations (17) and (18) indicates that the bending rigidity and the mass per meter of the strand can be obtained and listed as shown in Table 1.

Strand No.	Theoretical Tension T (kN)	Bending Rigidity EI $(kN{\cdot}m^2)$	Angle of Inclination α (°)	Length L (m)	Mass m (kg/m)
1st	1400	158.54	38	40	20.41
2nd	1200	158.54	38	40	20.41
3rd	1400	158.54	38	30	20.41
4th	1200	158.54	38	30	20.41

Table 1: Material parameters of the strand

Table 1 shows that the strands are classified into two different tensions and lengths. Therefore, the tension of a strand with different tensions and lengths can be studied.

The effectiveness of the proposed method is verified and compared by combining the given theoretical value and the results without considering bending rigidity (Xu and Huang, 2002). The tension of the strand was calculated according to the natural vibration frequencies of the top 10 orders, as shown in Table 2, where T_{fi} is the cable tension deduced from frequency f_i of order i^{th}.

Strand tension based on order of frequency	Calculation Method							
	Xu and Huang (2002) $T=\frac{4mL^2}{k^2}\cdot f_k^{\,2}$				Proposed method in Equation (14) $T=\frac{4mL^2}{k^2}\cdot f_k^{\,2}-\frac{k^2\pi^2}{L^2}\cdot EI$			
	1st	2nd	3rd	4th	1st	2nd	3rd	4th
T_{f1}	1418	1218	1424	1223	1417	1217	1422	1221
T_{f2}	1424	1223	1434	1232	1420	1219	1427	1225
T_{f3}	1433	1230	1447	1244	1424	1221	1431	1228
T_{f4}	1446	1241	1459	1261	1430	1225	1431	1233
T_{f5}	1449	1255	1472	1274	1425	1231	1429	1231
T_{f6}	1456	1269	1481	1276	1421	1234	1418	1213
T_{f7}	1453	1281	1473	1273	1405	1233	1388	1188
T_{f8}	1452	1280	1460	1272	1389	1217	1349	1161
T_{f9}	1442	1268	1451	1250	1363	1189	1310	1109
T_{f10}	1427	1253	1445	1228	1329	1155	1271	1054

Table 2: Comparison between calculation and analysis values of strand tension (kN).

Different calculation methods can be obtained by comparing the calculated value with the use of the two different methods in Table 2. The variations between the theoretical reference value and calculated value under different order frequencies are compared and shown in Figure 4.

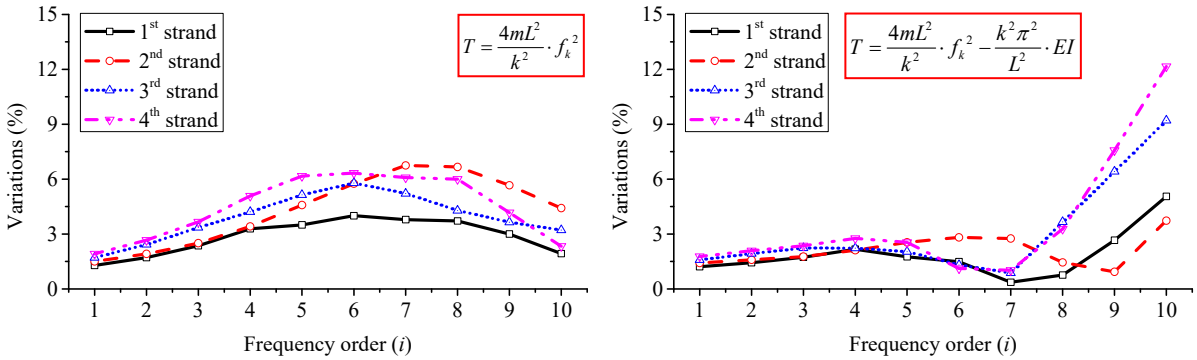

(a) Proposed Method by Xu and Huang [1]

(b) Proposed method in this paper

Figure 4: Comparison of variations with different methods.

A comparison between Table 1 and Figure 4 indicated that the calculated strand tensions according to the 1st and 10th frequencies varied significantly from the theoretical value shown in Table 2. However, according to the construction requirement for cable-supported bridges in the Chinese code (Wang et al., 2014), the permissible error of strand tension is 3%. Further investigation indicated that only the first and second orders of the frequency met the requirements simultaneously by using the method proposed by Xu and Huang (2002). Meanwhile, the order of the frequency from 1 to 7 meets the requirements for all of the four studied strands by adopting the method proposed as Equation (14) in this paper. Consequently, only the first two order frequencies can be used to calculate the strand tension by utilizing the method proposed by Xu and Huang (2002), which is suitable only for low-order frequency calculation. However, additional orders are provided for more options when the effect of bending rigidity is considered in the proposed method, which is suitable for low-order and high-order frequency calculations.

A comparison of Equation (14) and Figure 4 indicated that the effect of bending rigidity of the strand depends on the frequency order and the ratio of the first and second parts on the right side of Equation (14). The order of the frequency from 1 to 7 meets the requirements of this study when the parameters and tension of the strand are fixed, the order of k is high, and the variation is great; similar conclusions were obtained by Song et al. (2001). When the strand parameters are fixed, the tension, frequency, and relative value of the first part of Equation (14) decreases, and the effect of the bending rigidity of the strand increases. When the strand and tension parameters are fixed, the length decreases, the relative value of the second part of Equation (14) increases, and the effect of the bending rigidity of the strand increases. When the strand and tension parameters are fixed, the bending rigidity increases, the relative value of the second part of Equation (14) increases, and the effect of the second part increases.

4 APPLICATION ON NANXI YANGTZE BRIDGE

Nanxi Yangtze Bridge, located in southeastern China, is a single-span suspension bridge with a steel box and a stiffening girder with a main span of 820 m, as shown in Figure 5. The southern and

northern banks are the tunnel and gravity anchorages, respectively. The main cable consists of 87 strands, and each strand consists of 127-wire galvanized steel wires. The number of strands for the side span is 89. Some strands were taken as studied cases, as shown in Figure 6(a).

Figure 5: Layout of Nanxi Yangtze Bridge during construction.

During the construction of this bridge, only 12 high-precision pressure sensors were arranged in each anchor span for bridge construction monitoring, while nearly 100 strands need to be controlled. Thus, the tension of the strand in the anchor span is controlled by using a combination of string vibration method (see Figure 6) and pressure sensor method (see Figure 7) during construction. Field data could be acquired directly through the pressure sensor method, and that of the string vibration method could be calculated by using Equations (14) and (16).

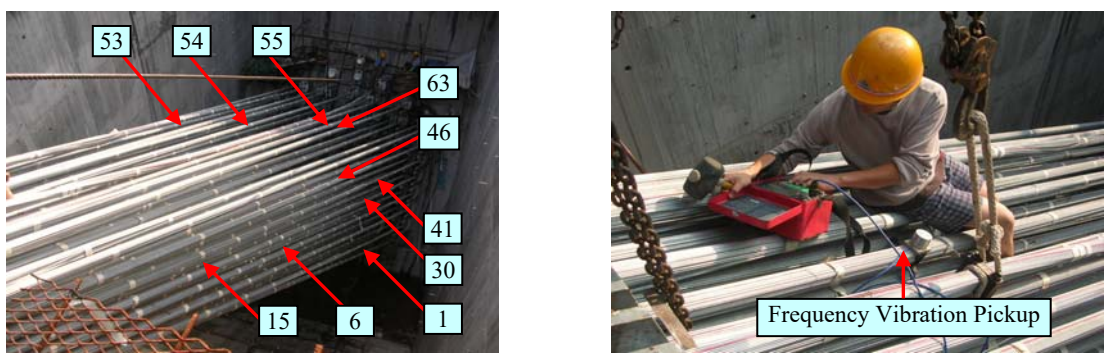

(a) Distribution of studied strands (b) Frequency testing in the field

Figure 6: Frequency testing of the studied strands in the anchor span.

During field testing, the temperature in the anchor span is stable, and the tension of the strand has a fixed value within a short time. However, in the indirect method, the value of the frequency test (see Figure 6(b)) always fluctuates, and the amplitude of fluctuation varies from –0.05 to 0.05 Hz. Thus, the frequency of the field test is the average of the three measure values for each tested

strand. In the direct method, the field tension of the strand T_1 is stable and unchanged because the temperature is stable within a short period, and the field data are recorded directly as strand tension T_1.

(a) Pressure sensors (b) Tension testing in the field

Figure 7: Tension testing of studied strands in the anchor span.

A comparison of the data obtained by the string vibration method, the pressure sensor method, and the theoretical value for the design is shown in Table 3. As indicated in Table 3, T_1 is the field value with arranged sensors, T_2 and T_3 are the calculated values derived by Equations (14) and (16) with consideration of the effect of the temperature, T_4 is the fitted value by T_2 and T_3, and T_5 is the true value of the design.

The effect of temperature on T_2 and T_3 can be indicated as follows:

$$\begin{aligned} \Delta T &= (t_t - t_d)\cdot\alpha\cdot EA \\ &= \Delta t\cdot\alpha\cdot EA \end{aligned} \tag{19}$$

where ΔT is the influence value of the tension for the strand by temperature variation, t_t is the temperature of field testing, t_d is the design reference temperature, ΔT is the value of the temperature variation, α is the coefficient of linear expansion, E is Young's modulus of the steel wire, and A is the area of the strand.

As shown in Table 3, T_1 is closest to T_5 and the difference between T_1 and T_5 is the smallest. The relative difference between T_2 and T_5 is larger than that of T_3 and T_5, which indicates that the boundary conditions significantly affect the results of the test and calculation through the frequency method. The boundary condition for the strand in the anchor span is neither hinged nor consolidated but in between. To further examine the situation of the boundary conditions, the variations under different order frequencies are calculated, as shown in Figure 8.

A comparison of Table 3 with Figure 7 indicates that the variations for T_1 and T_5 vary from 0.02% to 0.69%, from 6.37% to 7.70% for T_2 and T_5, and from 0.85% to 2.55% for T_3 and T_5. Evidently, the variations of T_2 and T_5 are larger than those of T_3 and T_5, and those of T_1 and T_5 are the smallest, indicating that the direct method using load measurement devices has the highest accuracy, followed by the method in Equation (14), whereas that of Equation (16) is the worst. The

accuracy of T_1 and T_2 satisfied the 3% requirement, whereas that of T_3 did not. This finding shows that the boundary conditions significantly affect the frequency method for the strand of the anchor span in suspension bridges, and the boundary conditions of the studied strands are fixed between hinged and consolidated. Further investigation is needed to determine whether the boundary conditions tend to hinge or consolidate needs.

Strand No.	Field data			Calculation data			Tension for design T_5 (kN)
	Frequency (Hz)	Temperature (°C)	Measured by pressure sensors T_1 (kN)	Calculated by Equation (14) T_2 (kN)	Calculated by Equation (16) T_3 (kN)	Fitted by least squares method T_4 (kN)	
1st	1.782	23.5	222.11	208.97	228.17	225.01	223.65
6th	1.772	23.4	222.82	206.2	225.25	222.10	222.87
15th	1.793	22.8	226.72	210.67	229.9	226.76	226.83
30th	1.763	24.3	218.52	203.25	222.12	218.99	218.71
41st	1.766	23.9	220.61	203.65	222.53	219.40	220.65
46th	1.731	25.7	210.38	194.56	212.96	209.86	210.55
53rd	1.672	28.4	196.13	181.51	199.31	196.22	196.34
54th	1.721	26.2	207.55	191.63	209.87	206.78	207.49
55th	1.72	26.8	202.88	191.28	209.49	206.41	204.29
62nd	1.66	28.9	193.71	179.17	196.86	193.77	193.91

Note: T_2 and T_3 have been revised according to Equation (19).

Table 3: Comparison of strand tensions

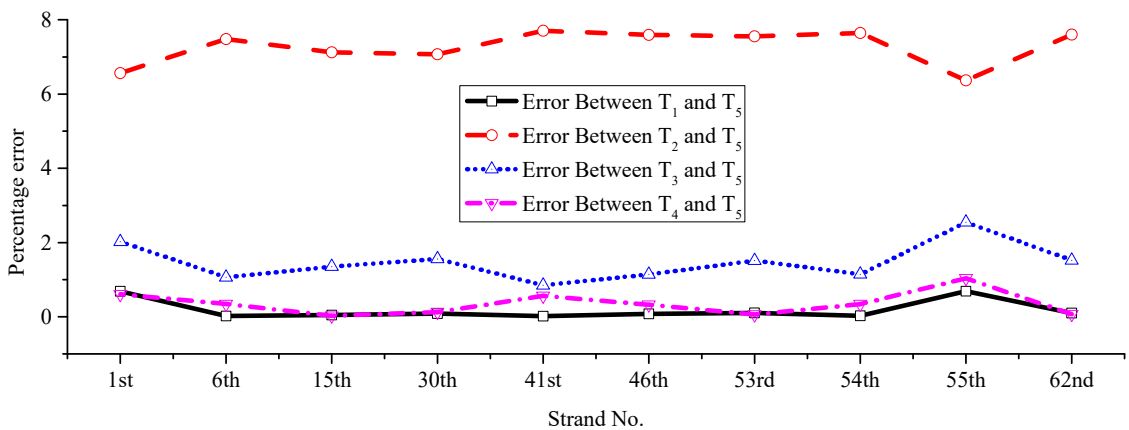

Figure 8: Comparison of variations between field, calculation, and designed data.

For clear and definite strand boundary conditions, the least squares method was introduced in the analysis of T_2 and T_3. By calculation, fitted value T_4 can be expressed by T_2 and T_3, i.e.,

$$T_4 = 0.3224\,T_2 + 0.6908\,T_3 \tag{20}$$

A comparison of the coefficients in Equation (20) indicates that the boundary conditions for the strand in the anchor span that tends to hinge has a 32% probability, and the boundary conditions for the strand in the anchor span that tends to consolidate has a 68% probability, which denotes that the boundary conditions significantly tend to consolidate. After fitting, strand tension T_4 can be obtained by Equation (20). The corresponding data items of T_2 and T_3, as shown in Table 3, and the variations of T_3 and T_5 can be determined and illustrated in Figure 7.

Based on Figure 8 and Table 3, the variations of T_4 and T_5 vary from 0.03% to 1.04% and the average variation is 0.35%. The accuracy of the tension control of the strand in the anchor span can be significantly improved using the least squares method. A comparison of T_1 and T_4 shows that the fitted value T_4 is very close to the measured value T_1 by the pressure sensors, and the average value of the variation for T_1 and T_5 is 0.19%, which implies that T_4 is almost as accurate as T_1.

5 CONCLUSIONS

In this paper, a new calculation method for strand tension is explored by using dynamic balance theory to determine the effect of bending rigidity and boundary conditions. Comparative studies are conducted using the proposed method for strand tension control with the examples and field data. The following conclusions are obtained:

1. In the frequency method, only the low-order frequency calculation can be considered to calculate the strand tension without considering the effect of bending rigidity to ensure control accuracy. If the effect of bending rigidity is considered, the high-order frequency calculation can be used to calculate the strand tension with high accuracy.
2. The influence of bending rigidity depends on the value of internal tension, strand length, and value of bending rigidity. For the strand of the anchor span in a suspension ridge and a similar strand, the length is short and the internal tension is low. Under this condition, the effect of bending rigidity is significant and its effect should be considered.
3. During strand construction in the anchor of a suspension bridge, the strand tension always starts from a low-stress to a high-stress state. For tension control accuracy, the effect of bending rigidity must be considered in the initial low-stress phase, whereas the project requirements must be considered in the late high-stress phase.
4. The boundary conditions of the strand significantly affect the calculation results. The boundary conditions of the strand in the anchor span are between hinged and consolidated, with an inclination to consolidate.
5. Under incomplete and inexplicit boundary conditions, the proposed least squares method is an effective, direct, and economical choice to improve the tension control accuracy of the strand in the suspension bridge anchor.

Acknowledgments

The research described in this paper was financially supported by the National Basic Research Program of China (973 Program, 2015CB057701), the Natural Science Foundation of China (51308071, 51378081), the Natural Science Foundation of Hunan Province (13JJ4057), the Foundation of China Scholarship Council (201408430155), and the Traffic Department of Applied Basic Research Project (2015319825120).

References

Cho, S., Yim, J., Shin, S. W., Jung, H. J., et al., (2012). Comparative field study of cable tension measurement for a cable-stayed bridge. Journal of Bridge Engineering 18(8): 748-757.

Choi, D. H., Park, W. S., (2011). Tension force estimation of extradosed bridge cables oscillating nonlinearly under gravity effects. International Journal of Steel Structures 11(3):383-394.

Fang, Z., Wang, J. Q., (2012). Practical formula for cable tension estimation by vibration method. Journal of Bridge Engineering 17(1):161-164.

Geier, R., De Roeck, G., Petz, J., (2005). Cable force determination for the Danube channel bridge in Vienna. Structural engineering international 15(3): 181-185.

Hua, X. G., Ni, Y. Q., Chen, Z. Q., (2009). Structural damage detection of cable-stayed bridge using changes in cable forces and model updating. Journal of Structural Engineering 135(9):1093-1106.

Kreis, E. S., Andre, J. C., (2005). A numerical inquiry into the flutter phenomenon in long-span bridges. Latin American Journal of Solids and Structures 2(4): 321-337.

Li, G. Q., Wei, J. B., Zhang, K. Y., (2011). Theoretical and experimental study for cable tension estimation by vibration method accounting for flexural stiffness and flexibility support. China Civil Engineering Journal 44(3):79-84.

Liu, J., Liu, K., (2010). Application of an active electromagnetic vibration absorber in vibration suppression. Structural Control and Health Monitoring 17(3): 278-300.

Loh, C. H., Chang, C. M., (2006). Vibration control assessment of ASCE benchmark model of cable-stayed bridge. Structural Control and Health Monitoring 13(4): 825-848.

Loh, C. H., Chang, C. M., (2007). MATLAB-based seismic response control of a cable-stayed bridge: cable vibration. Structural Control and Health Monitoring 14(1): 109-143.

Ni, Y. Q., (2002). Dynamic analysis of large-diameter sagged cables taking into account flexural rigidity. Journal of Sound Vibration 257(2):301-319.

Ricciardi, G., Saitta, F. (2008). A continuous vibration analysis model for cables with sag and bending stiffness. Engineering Structures 30(5):1459-1472.

Riceiardi, G., Saitta, F., (2008). A continuous analysis model for cables with sag and bending stiffness. Engineering Structures 30(2):1459-1472.

Song, Y. F., He, S. H., Wu, X. P., (2001). Energy method of the tension for fixed-end rigid cables. Journal of Xi'an Highway University 21(1): 55-57. (in Chinese)

Wang, D., Deng, J., Chen, C. M., et al., (2015). Analysis of calculation parameters influence on anchor span strand tension for long-span suspension bridge. Journal of Highway and Transportation Research and Development 32(1): 63-68. (in Chinese)

Wang, D., Li, Y. P., Liu, Y., (2014). Analysis of the intelligent control of anchor span tension for long-span suspension bridge. China Journal of Highway and Transport 27(1):51-56. (in Chinese)

Xu, H. Z., Hung, P. M., (2002). Cable tension control in anchorage span of suspension bridge. Journal of Xi'an Highway University 22(5): 32-34. (in Chinese)

Yau, J. D., (2013). Wave passage effects on the seismic response of a maglev vehicle moving on multi-span guideway. Latin American Journal of Solids and Structures 10(5): 981-1000.

Ye, X. J., Yan, Q. S., Li, J., (2012). Modal identification and cable tension estimation of long span cable-stayed bridge based on ambient excitation. Journal of Vibration and Shock 31(16): 157-163.

Zuo, X. B., Li, A. Q., (2011). Numerical and experimental investigation on cable vibration mitigation using shape memory alloy damper. Structural Control and Health Monitoring 18(1): 20-39.